

Soft Matter

Accepted Manuscript



This is an *Accepted Manuscript*, which has been through the Royal Society of Chemistry peer review process and has been accepted for publication.

Accepted Manuscripts are published online shortly after acceptance, before technical editing, formatting and proof reading. Using this free service, authors can make their results available to the community, in citable form, before we publish the edited article. We will replace this *Accepted Manuscript* with the edited and formatted *Advance Article* as soon as it is available.

You can find more information about *Accepted Manuscripts* in the [Information for Authors](#).

Please note that technical editing may introduce minor changes to the text and/or graphics, which may alter content. The journal's standard [Terms & Conditions](#) and the [Ethical guidelines](#) still apply. In no event shall the Royal Society of Chemistry be held responsible for any errors or omissions in this *Accepted Manuscript* or any consequences arising from the use of any information it contains.

Cite this: DOI: 10.1039/c0xx00000x

www.rsc.org/xxxxxx

ARTICLE TYPE

Thermal fluctuations in chemically cross-linked polymers of cyclodextrins

Barbara Rossi^{*a}, Valentina Venuti^b, Alessandro Paciaroni^c, Andrea Mele^d, Stéphane Longeville^e,
Francesca Natali^f, Vincenza Crupi^b, Domenico Majolino^b and Francesco Trotta^g

⁵ Received (in XXX, XXX) Xth XXXXXXXXX 20XX, Accepted Xth XXXXXXXXX 20XX

DOI: 10.1039/b000000x

The extent and the nature of thermal fluctuations in the innovative class of cross-linked polymers called cyclodextrin nanosponges (CDNS) are investigated, on the picosecond time scale, through elastic and quasielastic neutron scattering experiments. Nanosponges are complex 3D polymer networks where covalent bonds connecting different cyclodextrin (CD) units and intra- and intermolecular hydrogen-bond interactions cooperate to define the molecular architecture and fast dynamics of the polymer. The study presented here aims to clarify the nature of conformational rearrangements activated by increasing temperature into the nanosponge polymer and the constraints imposed by intra- and intermolecular hydrogen-bond patterns on the internal dynamics of the macromolecule. The results suggest a picture in which the conformational rearrangements involving the torsion of the OH groups around the C-O bonds dominates the internal dynamics of the polymer over the picosecond time-scale. Moreover, the estimated values of mean square displacements reveal that the motions of the hydrogen atoms in the nanosponges are progressively hampered as the cross-linking degree of the polymer is increased. Finally, the study of the molecular relaxations suggests a dynamical rearrangement of the hydrogen-bond networks characterized by a jump diffusion motion of more mobile hydrogen atoms belonging to the OH group of CD units. All these findings add a further contribution to the rational comprehensive view of the dynamics of these macromolecules resulting particularly beneficial in designing new drug-delivery systems with tuneable inclusion/release properties.

Introduction

The use of cross-linked polymer for smart applications in technological fields of high social impact is presently attracting great attention¹. As a matter of fact, cross-linked polymers have been shown to be superior in uses requiring resistance to high temperatures and high mechanical performance¹. Polymeric networks of molecules are considered a very versatile class of materials with tailored properties at different length scales and they are proposed in the fast-growing field of drug delivery, tissue engineering, and regenerative medicine²⁻⁴.

In this perspective, cyclodextrin nanosponges (CDNS) play a relevant role in the design and development of new delivery systems adapted to the physicochemical features of the actives and the therapeutic demands of the pathology⁵⁻⁶. In particular, they offer the interesting possibility to selectively encapsulate and release both hydrophobic and hydrophilic active ingredients⁵⁻¹².

Nanosponges are prepared by poly-condensation between cyclodextrins (CD) – cyclic oligomers of amylose well known for their ability to form inclusion complexes with a large variety of guest molecules^{13,14} – and suitable cross linking agents (CL), such as carbonyldiimidazole (CDI)^{15,16}, pyromellitic anhydride (PMA)¹⁷⁻²³ or activated derivatives of ethylenediaminetetraacetic acid (EDTA)²⁴⁻²⁶. The reaction of polymerization leads to the formation of a three-dimensional network of CD units showing both hydrophilic and hydrophobic nano-sized cavities (Figure 1(a)). X-ray diffraction¹⁸ and low-frequency inelastic light¹⁷ and neutron²³ scattering measurements indicate that cyclodextrin nanosponges are, in the majority of cases, completely amorphous, making a thorough structural characterization a still open investigation field.

These polymers are safe and biodegradable material with negligible toxicity on cell cultures and they are considered to

exhibit superior inclusion ability with respect to native CD by incorporating a large class of molecules within their structure⁵.

Some types of CDNS exhibit a marked swelling behaviour in the presence of aqueous solution, giving rise to the formation of gel-like dispersion^{20-22,25-27}. This ability to absorb a large amount of water is particularly intriguing in view of the possible use of these polymeric matrices as efficient water nano-containers²⁷. Moreover, the hydrogels obtained by swelling of CDNS polymers seem to be good candidates as stimuli-responsive systems for the entrapment/release of bio-active compounds. It was shown that their physical state can be modified in a controlled way^{22,25,26,27}, and allowed to pass progressively from a rigid gel to a liquid suspension upon gradual increase of the hydration level of CDNS in water.

The functional features of CDNS, such as their water holder capacity and inclusion/release capabilities, are intimately related to the molecular structure and conformational rearrangements of the chemical groups within the cross-linked network. In this sense, a full explanation of the relationship existing between molecular architecture and polymer dynamics in CDNS and their corresponding macroscopic physical properties is still an ambitious objective to be reached.

In recent years, many efforts have been devoted to explore the structural features of nanosponges over different length scales by implementing a broad repertoire of experimental and computational techniques. In particular, in the case of ester-bridged CDNS¹⁷⁻²⁶, previous results indicate that a crucial contribution to the molecular architecture and rigidity of the whole polymer network is given by the complex interplay between covalent bonds and non-covalent interactions – typically hydrogen bonds (HB) – connecting the CD units within the polymer^{20,23}. The connectivity pattern of these chemical-physical interactions have been explored in depth by a detailed analysis of the vibrational dynamics of CDNS performed in different

frequency regimes^{17,19,21,24,25} and by exploiting the different sensitivity of complementary techniques, such as inelastic light and neutron scattering²³. All the experimental results, clearly evidenced that the polymeric structure and the physical-chemical properties of CDNS can be successfully modulated by varying i) the chemical structure of CL¹⁷, ii) the type of CD²⁸ and iii) the relative amount of CL^{17,19,23,24,28} with respect to the monomer (i.e. n =molar ratio between cross-linking agent and CD). Among these factors, the molar ratio n mainly influences the degree of reticulation of the polymer during its synthesis, as demonstrated in our previous works^{17-20,23,24,28}. In these papers, an interpretation of the effect of the increasing amount of cross linking agent with respect to the monomer cyclodextrin on CDNS structure was proposed (Figure 1(b)). The cross-linking degree of the polymer grows with increasing molar ratio n up to a critical value beyond which further excess of CL results in the branching of the CD units rather than grafting them together, reasonably for steric crowd reasons.

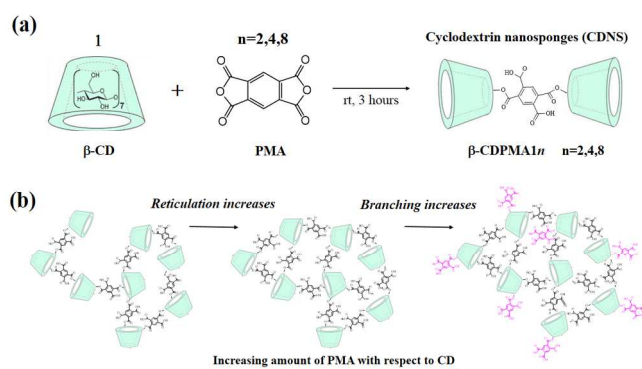


Figure 1: (a) Scheme of the synthesis of β -CDPMA $1n$ nanosponges by using PMA as cross-linking agent and β -CD as monomer. The scheme indicates the relative mole amounts of β -CD (1 mole, for clarity) and PMA (three different preparations: $n=2$, $n=4$ and $n=8$). Accordingly, three different types of CDNS are obtained. The full acronym β -CDPMA $1n$ thus indicates the polycondensation process between CD and PMA affording the corresponding nanosponge with starting molar ratios CD:PMA=1: n . For graphic clarity, the picture shows the formation of a dimer only. (b) Schematic picture of the effect of the increasing amount of PMA with respect to cyclodextrin monomer β -CD on CDNS structure. The cross-linking degree increases up to a maximum value, then further excess of PMA causes branching of CD units rather than further cross-linking.

In this work, we report the results of an extensive investigation on ester-bridged nanosponges dynamics over the picosecond temporal windows, by exploiting the potentiality of incoherent neutron scattering. As a matter of fact, elastic (ENS) and quasielastic (QENS) neutron scattering are among the most powerful experimental techniques to fine estimate the extent of the thermal fluctuations due to the molecular motions and the relaxational features in complex macromolecules. In particular, due to the energy resolution of the neutron scattering spectrometers employed in the present study, the attention will be focussed on the dynamical processes involving the fluctuation of the hydrogen-bonds networks formed inside a single CD molecule (intra-molecular HB) and among different CD units (inter-molecular HB). The dynamics of PMA-nanosponges obtained by polymerization of CD with pyromellitic anhydride at different values of molar ratio n is investigated, as a function of temperature, and compared with the characteristic internal motions of the monomeric unit β -cyclodextrin. Interestingly, a general increase of the cyclodextrin OH group

mobility is observed when CD units are assembled into the polymeric network of CDNS. Moreover, the analysis of the elastic incoherent structure factor suggests a model of atomic motions which is well described by a random jump diffusion of hydrogen atoms into the HB patterns involving the OH groups of CD.

These results add a further contribution to the rational comprehensive view of the fast dynamics of CD assembled in CDNS network and could be particularly beneficial in designing new stimuli-responsive CDNS hydrogel with tuneable inclusion/release properties.

Materials and methods

A Synthesis and purification of nanosponges

The ester-bridged cyclodextrin nanosponges based on pyromellitic anhydride were obtained by following the synthetic procedure already described in the Italian patent with minor modification²⁹⁻³¹.

In order to obtain the β -CDPMA $1n$ polymers (for the notation see Figure 1(a)), the reactions of polymerization between β -CD and the cross-linking agent pyromellitic dianhydride (PMA) at β -CD:PMA molar ratios of 1: n (with $n = 2, 4, 8$) were conducted by dissolving the reagents in dimethyl sulfoxide (DMSO) in the presence of triethylamine and allowing them to react at room temperature for 3 hours. Once the reaction was over, the solid obtained was broken up with a spatula and washed with acetone in a Soxhlet apparatus for 24 hours. This process ensures the complete removal of unreacted reagents and the purification of the final polymer product. The pale yellow solid material was finally dried under vacuum for about 24 hours, which is generally a time sufficient to achieve a constant weight of the product. After the drying procedure, no further water is present or can be removed. The chemical and thermal stability of nanosponges have been previously evaluated⁵ and the results indicate that a degradation of material is observed only at high temperature values ($>60^\circ\text{C}$) in acid conditions.

B Neutron scattering experiments

Quasi elastic neutron scattering experiments were performed at Laboratoire Léon Brillouin (LLB, Saclay, France) using the time-of-flight (TOF) spectrometer MIBEMOL.

Measurements were carried out at temperature of 150 and 300 K using neutrons with an incident wavelength of 6 Å, with a Q-independent experimental elastic energy resolution of 92.7 μeV (defined as the full-width half-maximum of a vanadium standard FWHM). The covered Q-range was from 0.49 \AA^{-1} to 1.73 \AA^{-1} . The recorded spectra have been binned into 10 groups to improve the counting statistics. The explored energy range was from -45 meV to about 1.4 meV. In all of the figures here reported the sign of the energy transfer has been reversed for sake of simplicity. As sample holder, a standard, indium sealed, flat aluminum cell, with a thickness of 0.2 mm internal spacing was used. For each measurement, the sample holder was placed at an angle of 135° with respect to the incident beam direction. The time of data acquisition was about 8 hours. A transmission of $\sim 96\%$ was estimated for all the investigated samples. The measured time-of-flight spectra were analyzed with QENSH data treatment program, available at LLB, that allows, *inter alia*, the correction of the detector efficiency by normalization to vanadium spectra, the correction for the empty cell, the transformation of the TOF spectra into energy spectra, and the data grouping to improve the corresponding signal/noise ratio.

Elastic scattering scans were performed by using the high-energy

resolution, wide momentum transfer backscattering spectrometer IN13, at the Institut Laue-Langevin (ILL, Grenoble, France). An energy resolution of 9 μeV FWHM, corresponding to an incident neutron wavelength of 2.23 \AA , were achieved in the Q range 0.2–4.6 \AA^{-1} . As sample holder, a standard, indium sealed, flat aluminium cell with a thickness of 0.3 mm was used for all the examined samples. The temperatures explored ranged from 130 to 310 K and an acquisition time variable between 1 and 2 hours depending on the type of nanosponge. The acquired data were corrected in order to take into account the incident flux, cell scattering, self-shielding, and detector responses. Then, the elastic intensity of each sample relative to a given temperature was normalized with respect to the corresponding lowest measured temperature ($T=20\text{K}$). A transmission of about 90% was measured for β -CDPMA12, of 88% for β -CDPMA14 and of 88.5% for β -CDPMA18. The data have not been corrected by the multiple scattering contribution, which is estimated to be below 10% on the elastic peak and affects in a very similar way all the analysed samples.

C Theoretical background

In a typical neutron scattering experiment, the molecular motions of the atoms are investigated by measuring the so-called dynamical structure factor $S(Q, E)$ which gives the probability that an incident neutron is scattered by the sample with an energy E and an exchanged momentum Q . The functional dependence of $S(Q, E)$ on E and Q provides information, respectively, on the characteristic time scales and the geometry of the molecular motions that contribute to the revealed signal. The dynamical structure factor includes both coherent and incoherent contributions, which arise from, respectively, inter- or self-particle correlations of collective or individual atomic motions. However, in the case of samples under investigation in our experiment, the dominant contribution to the revealed signal is due to the large amount of hydrogen atoms, characterized by a very large, almost exclusively incoherent neutron cross section³². Therefore, neutron scattering experiment allows us to study the self-particle dynamics of hydrogen atoms which can be considered as a probe of the thermal fluctuations of the whole molecule.^{33–36}

In the incoherent approximation, the intensity of scattered neutrons can be written, at a given temperature T , as:

$$S(Q, E) = e^{-2W(Q, T)} \{A_0(Q)\delta(\omega) + [1 - A_0(Q)]S_{QE}(Q, \omega) + S_{INEL}(Q, \omega)\} \otimes R(Q, \omega) \quad (1)$$

The term $A_0(Q)\delta(\omega)$ in eq. (1) represents the elastic response of the system, due to those scattering events which do not involve change in energy, while the function $S_{QE}(Q, \omega)$ is the quasielastic scattering contribution which gives information about the diffusive and relaxational motions of the system. Finally, the term $S_{INEL}(Q, \omega)$ represents the inelastic scattering part of the spectra which is usually much less intense than the quasielastic contribution and it is modelled with a flat background. All the internal motions are convoluted with the experimental resolution function $R(Q, \omega)$.

1. Analysis of the elastic intensities

The term $e^{-2W(Q, T)}$ which appears in eq. (1) is the so-called Debye-Waller factor which describes the Q -dependence of the elastic intensity due to the vibrational atomic mean-square displacement (MSD) $\langle u^2 \rangle$. In the Gaussian approximation this factor can be written as $e^{-2W(Q, T)} = e^{-(u^2)Q^2}$.

The energy dependence of the elastic signal is described by a delta function $\delta(\omega)$ whereas the modulation as a function of Q is provided by the elastic incoherent structure factor (EISF) $A_0(Q)$,

that is the space-Fourier transform of the scatterers distributions taken at infinite time, averaged over all the possible initial positions. The Q -behaviour of the factor $A_0(Q)$ provides information on the geometry and type of motions of the scattering centres. As we will see below, the measured elastic intensity shows a non-Gaussian Q -dependence more and more visible as the temperature increases, while the quasielastic linewidths display a Q -independent trend. This behaviour suggests that the neutron scattering signal originates from an anharmonic dynamics, possibly involving random jump confined motions. A quite reasonable model to describe these dynamical features is the so-called double-well model,³⁸ extensively applied to picosecond proton dynamics in several kinds of disordered systems.^{39,40} It provides an over-simplified description of the energy landscape, taking into account the deviation of the elastic intensity from the Gaussian behaviour. In spite of this approximation, one can obtain, as explained in the following, a quantitative estimation of the mean square displacements. In this framework, the protons are considered dynamically equivalent, and their motions are schematized as jumps between two distinct sites with a free energy difference ΔG .

On the basis of the double-well jump model, the corresponding EISF can be written as⁴¹:

$$A_0(Q) = 1 - 2p_1p_2 \left(1 - \frac{\sin Qd}{Qd}\right) \quad (2)$$

where p_1 and $p_2 = (1 - p_1)$ are the occupation probabilities of the ground and the excited state, and d defines the spatial distance between the two potential wells.

In the harmonic approximation the temperature-dependence of $\langle u^2 \rangle$ in the Debye-Waller factor can be described by using the Einstein model of independent quantized oscillators³⁴:

$$\langle u^2 \rangle = \frac{\hbar\omega}{2K} \coth\left(\frac{\hbar\omega}{2K_B T}\right) - \langle u^2 \rangle_0 \quad (3)$$

in which K and ω represent, respectively, the average force field constant and the average frequency of the set of the oscillators; accordingly, the relationship $\langle u^2 \rangle_0 = \hbar\omega/2K$ provides the zero-point mean square displacements.

Actually, since the measured elastic intensity has been normalized with respect to the lowest temperature (as indicated below), the zero-point mean square displacements have been subtracted in the right side of eq. 3.

Finally, a quantitative measurement of the average hydrogen mobility is given by the total MSD $\langle u^2 \rangle_{tot}$ which can be derived from eq. 1, with $A_0(Q)$ given by eq. 2 and $\langle u^2 \rangle$ given by eq. 3, through the relationship³⁷:

$$\langle u^2 \rangle_{tot} = \left[\frac{d \ln S(Q, E \approx 0)}{d(Q^2)} \right]_{Q=0} = \langle u^2 \rangle + \frac{1}{3}p_1p_2d^2 = \langle u^2 \rangle + \langle u^2 \rangle_c \quad (4)$$

In the above equation, $\langle u^2 \rangle$ is the aforementioned harmonic vibrational MSD term, while $\frac{1}{3}p_1p_2d^2 = \langle u^2 \rangle_c$ represents the conformational contribution to the total MSD⁴⁰ which describes the proton mobility due to jumping between the two energetic sites.

2. Analysis of the quasielastic contribution

Due to the complexity of the structure of the systems under investigation, many different kinds of motions can give rise to quasielastic signal $S_{QE}(Q, \omega)$ in eq. (1). On one side, the movements of the highly diversified molecular subunits produce quite different quasielastic contributions. On the other side, even identical subunits may experience different local environments and thus move in different ways. For these reasons, it is therefore very difficult to find an exact theoretical function to describe the quasielastic signal.

It is then more useful to model the term $S_{QE}(Q, \omega)$ through a phenomenological function described as a sum of Lorentzians curves^{42,43}:

$$[1 - A_0(Q)]S_{QE}(Q, \omega) = \sum_n QISF_n(Q)L_n(\sigma_n, \omega) \quad (5)$$

where $L_n(\sigma_n, \omega)$ is the n -th Lorentzian function, σ_n is its FWHM, the inverse of which provides an estimate of the characteristic time scale of the corresponding motion and $QISF_n(Q)$ is the quasielastic incoherent structure factor which provides the energy integral of the n -th quasielastic component and quantifies the degree of activity of the relevant motion. As a matter of fact, the dynamical heterogeneity of the hydrogen atoms in the system gives rise to a variety of quasielastic components in the spectra and every Lorentzian function represents, rather than a single kind of movement, a broad, almost continuous distribution of motions, each characterized by its own correlation time and related linewidth. Thus, in this context, it should be regarded as an “effective” linewidth, whereas should be considered as a quantitative measure of the activated dynamical processes.

20 Results and discussion

A Conformational mobility of OH groups

In Figure 2(a)-(b), the incoherent elastic neutron scattering intensities measured for β -CDPMA12 and β -CDPMA14 nanosponges are shown, as a function of Q^2 , at three different values of temperature T . The experimental profiles are reported after the usual standard corrections and normalization (see section Materials and Methods).

The logarithmic scale in Fig. 2 allows us to point out that the experimental elastic intensities exhibit a Q^2 dependence that tends to slightly depart from the Gaussian-like behaviour of the Debye-Waller factor. This effect, which becomes more and more pronounced as the temperature increases, has been already revealed in other systems like hydrated protein powders^{44,45} and cyclodextrin inclusion complexes⁴⁶. In these systems the departure from the Gaussian dependence has been interpreted as originating from anharmonic motions, involving the re-orientational dynamics of small molecular groups, and described in terms of the double-well model³⁸. We may expect that a similar dynamical activation can be at the basis of the behaviour found in the present systems, due to the significant contribution from the re-orientations of OH groups belonging to both cyclodextrin and cross-linking agent. This is why we chose to describe the experimental elastic intensities by using the double-well model^{38,41,44,46}, according to the equation:

$$S(Q, \omega \approx 0) \propto e^{-(u^2)_G Q^2} [A_0(Q)\delta(\omega)] \otimes R(Q, \omega) \quad (6)$$

where $A_0(Q)$ and $(u^2)_G$ are given by eq. (2) and (3), respectively.

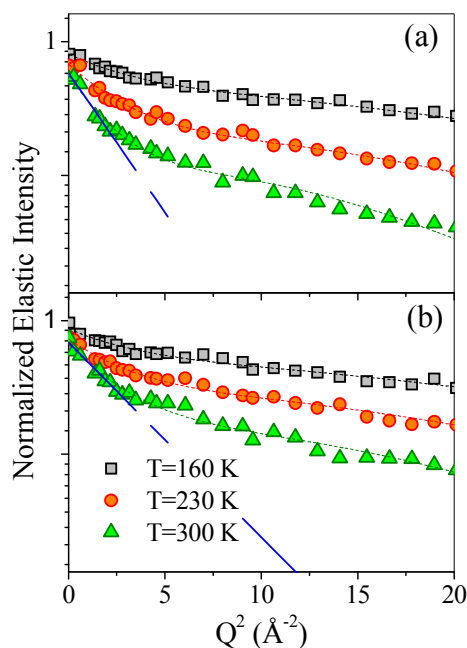


Figure 2: Normalized incoherent elastic intensities as a function of Q^2 for (a) β -CDPMA12 and (b) β -CDPMA14 nanosponges at three different temperatures. Experimental data (open symbols) are reported together the fit (dashed line) according to eq. (6) (see text for details). The blue lines highlight the change of slope typical of a non-Gaussian behaviour. The error bars (less than 15%) are not reported for sake of clarity.

Equation (6) provides an excellent fit to the data, as shown in Fig. 2, with a jump distance d equal to 1.7 ± 0.2 Å for all the analysed samples of nanosponges, independent of the temperature.

Since the measured elastic intensity reflects the dynamical contribution of the motions of atoms of CDNS that are accessible in the experimental energy and momentum transfer range, then the double-well jump model may provide only an average description of the internal dynamics of the polymers. In this context, our experimental data seem to suggest the existence of hydrogen atoms motions which are characterized by a spatial distance d . This internal dynamic may be related to reorientational degrees of freedom involving the hydrogen atoms of the several OH groups present in the polymeric framework and that easily undergo conformational rearrangements due to the torsion around the C-(OH) chemical bonds.

As a matter of fact, the value of the d parameter is consistent with the characteristic distance explored by the hydrogen atoms of OH groups during their reorientational motions. The temperature independence of this parameter suggests also that, as temperature increases, the extent of these torsional motions stays the same while the number of mobile OH groups progressively rise, as it is witnessed by the trend of the MSD shown in the next section. We can speculate that the increasing mobility on increasing the temperature and decreasing the cross-linking degree could be related to an improved effectiveness for particular purposes, such as inclusion of small molecules.

B Effect of hydrogen-bonds on internal polymer dynamics

As previously specified, quantitative information on the average proton dynamics of the system can be provided from the temperature-behaviour of the total mean square displacements $(u^2)_{tot}$. The total MSD, as obtained from eq. (4) (upper part) for the three different types of examined β -CDPMA1 n nanosponges

and for pure β -CD⁴⁶, are reported in Fig. 3 as a function of temperature.

It is noteworthy that, over the whole range of temperatures explored, the proton mobility of nanosponges is significantly higher than that of the monomeric unit β -CD. As we expect that a large contribution to the measured MSD comes from OH groups of cyclodextrins, this finding strongly suggests that the assembly of CD units into the polymeric network of CDNS gives rise to a general increase of the OH group degrees of freedom. To explain this effect, a picture can be proposed where the average mobility at a local level is increased due to the perturbation of the strongly interconnected intra-molecular hydrogen-bond (HB) network involving the 2- and 3-OH groups around the bottom rim of the cyclodextrin, as a consequence of the distortions of the CD macro-ring brought about by the polymerization process. This interpretation is consistent with the finding, previously reported by ¹³C CP-MAS NMR spectroscopy¹⁶ that the primary OH groups of CD are the principal reactive sites for the ester formation, thus leaving the majority of the OH groups in position 2 and 3 of the glucose units unreacted.

The findings described above can be related to the results of the inspection of the vibrational band observed in the IR spectra of CDNS in the high-wavenumber region and assigned to the stretching modes of the OH groups of the polymer¹⁹. The analysis of the spectral features of this complex band gives important information on the connectivity pattern of HB network of the system. Recent IR measurements performed on CDNS in dry state¹⁹ evidenced a disruption of the intra-molecular H-bond network at the larger rim of the CD units that was related to the increased steric hindrance of the whole system with growing cross-linking degree of nanosponges. This effect on the OH group populations of polymeric matrix was found to be largely dependent on the chemical nature of the cross-linker, as shown by the analysis of the vibrational spectra of CDI-based nanosponges¹⁵.

As a general trend, the mobility increase of the hydrogen atoms is observed for all the three types of β -CDPMA1*n* nanosponges with increasing temperature (Fig. 3). This finding seems to be consistent with our previous IR measurements^{15,19} that give evidence of a characteristic destructuring effects on the HB scheme in CDNS when the temperature of the polymer increases.

The comparison between the temperature-behaviour exhibited by the total MSD for the monomeric unit β -CD⁴⁶ and the nanosponge polymers (Fig. 3) deserves some specific comments. While the trend shown by the $\langle u^2 \rangle_{tot}$ of β -CDPMA12 nanosponges looks similar to that observed for pure β -CD, the temperature-dependence of MSD seems to change passing from *n*=2 to 8. The behaviour suggests that the polymeric systems become less temperature-responsive as increasing the molar ratio *n*, in agreement with the increasing constraint experienced by the OH groups in the nanosponge network. This finding appears of particular interest also in view of the possible potential applications of nanosponges as stimuli-responsive systems.

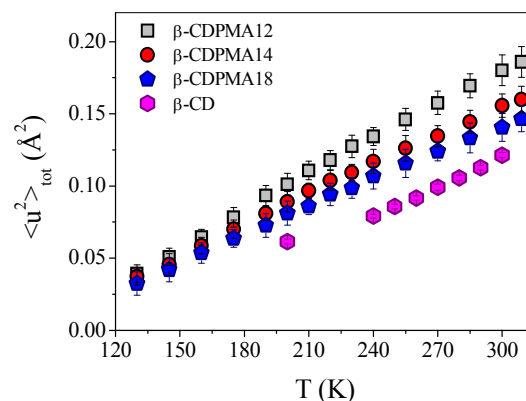


Figure 3: Total mean square displacements $\langle u^2 \rangle_{tot}$ as a function of temperature T for β -CDPMA1*n* nanosponges (*n*=2, 4 and 8) and β -CD [data from ref.⁴⁶].

C Mobility versus elastic constants

The values of MSD reported in Fig. 3 also point to a general hindering of the proton mobility of CDNS as the molar ratio *n* increases from 2 to 8. This result suggests that the parameter *n* strongly affects the internal polymer dynamics of CDNS on the picosecond time scale.

The behaviour found for MSD is fully consistent with the attenuation of the intensity of the vibrational modes of the CDNS polymer which is observed in the inelastic neutron scattering spectra²³. The vibrational density of states estimated for β -CDPMA1*n* nanosponges shows that the hydrogen atoms tend to exhibit vibrational motions of smaller amplitude when they are inserted in a more interconnected pattern of cross-links.

A more quantitative description of this effect can be provided by the estimation of the average rigidity of the samples in the high-temperature regime, where large structural fluctuations take place and the systems become less and less stable. It may be argued that, as the systems approach the instability region, the double-well method would lose its validity as the atoms will tend to explore most of the conformational space accessible to them. In this approximation, we can consider that in the high-T range, the energy landscape accessible to the hydrogen atoms will resemble a confining harmonic potential well⁴⁰:

$$V(r) = br^2/2 \quad (7)$$

This approximation holds provided that the experimental time-window is quite large, in such a way that the atoms have the time to explore the conformational landscape. Moreover, we are confident that eq. (7) may be applied for temperatures such that $p_2/p_1 \geq 0.5$, i.e. above 280 K where the conformational landscape is rather homogeneously populated. Under these conditions, the configurational mean square displacements $\langle u^2 \rangle_c$ can be described by the relation⁴¹:

$$\langle u^2 \rangle_c = K_B T / 3b \quad (8)$$

where the parameter *b* provides a quantitative estimation of the rigidity of the polymer network.

It is noteworthy that a similar approach has already been exploited to describe the proteins dynamic features in terms of an effective force constant^{47,48}.

The fit of the experimental $\langle u^2 \rangle_c$ performed by using eq. (8) in the high-T range allows us to obtain a direct measurement of *b* for the three different samples of nanosponges under investigation, as reported in Table 1.

Type of nanop sponge	b (N/m)
β -CDPMA12	0.96 ± 0.02
β -CDPMA14	1.02 ± 0.02
β -CDPMA18	1.12 ± 0.02
β -CD	0.70 ± 0.03

Table 1: Values of rigidity b obtained for β -CDPMA1 n nanosponges ($n=2, 4$ and 8) and pure β -CD.

The stiffness of nanosponges, as quantified by the b parameter, increases on passing from $n=2$ to $n=8$. This estimation of the average rigidity of the CDNS polymers can be related to the qualitative evolution of the low-frequency vibrational modes observed in the inelastic light^{17,18,24,28} and neutron scattering²³ spectra of nanosponges. In these previous works, the modifications revealed in the frequency position of Boson peak (BP) for different types of CDNS and as a function of molar ratio n were found to be consistent with the trend observed for the Brillouin sound velocity measured on the same samples¹⁷. We remark that both BP and Brillouin peaks are spectroscopic features related to the transformation of the elastic constants of the material, the former on mesoscopic length-scale, the latter on a wider scale, extending up to hundreds of nanometers. The analysis of inelastic light and neutron spectra of PMA-nanosponges^{17,23} clearly shows that BP shifts toward higher wavenumbers by changing the parameter n from 2 to 8. This behaviour was explained by considering a general increasing of the average rigidity (stiffness) of the CDNS polymer matrix, in full agreement with the estimated values of the parameter b reported in Table 1.

These results strongly confirm the hypothesis that the extent of the covalent network, controlled by the cross-linking agent/cyclodextrin molar ratio n , induces a general modifications of the elastic properties of nanosponges polymers.

This finding appears of particular interest given that the functional properties of CDNS, like their swelling ability and inclusion/release performances, are expected to be strongly affected by the rigidity of the three-dimensional polymeric matrix.

D Relaxational dynamics: reorganization of HB network

Further information on the polymer dynamics of CDNS can be obtained by the analysis of the relaxational processes of the system as provided by quasielastic neutron scattering signal. No quasielastic contribution has been revealed for all the investigated nanosponges polymers at $T = 150K$, while at $T = 300K$ the quasielastic signal can be immediately recognized in the experimental profiles of Fig. 4, as a broadening of the elastic peak.

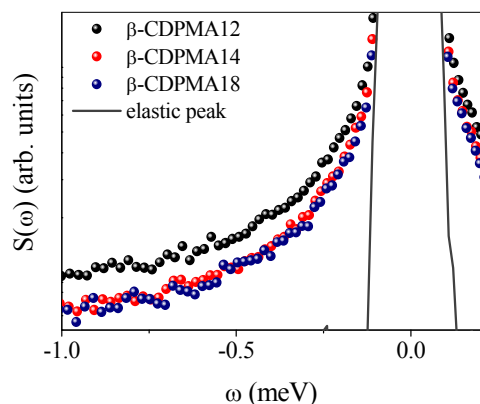


Figure 4: Lin-log plot of the normalized quasi elastic neutron scattering spectra of β -CDPMA1 n nanosponges ($n=2, 4$ and 8) at $T=300K$. The profiles have been obtained integrating the quasielastic intensities over the entire angular range. Symbols: experimental data; continuous line: elastic peak. The error bars (less than 10%) are not reported for sake of clarity.

The presence of the quasielastic contribution in the spectra of nanosponges suggests the existence of internal dynamics that can be related to the relaxation of the hydrogen bonds pattern involving the OH groups of CD units⁴⁹ in the polymer network of CDNS.

By inspection of the spectra in Fig. 4, it can be seen that the intensity of the quasielastic wings seems to decrease on passing from the $n=2$ to the $n=4,8$ values. The same qualitative behaviour was observed in the low-frequency Raman spectra of nanosponges^{24,28}, where the quasielastic contribution to the total experimental profiles varies passing from its maximum intensity at $n=2$ to the minimum one for high values of n . This trend is consistent also with the spectral modifications of BP observed in the inelastic light and neutron scattering spectra^{17,24,23,28} and with the estimation of the rigidity of the polymer matrix of CDNS reported in Table 1.

The trend shown in Fig. 4 could be due to either the narrowing of the quasielastic contribution (i.e. slower characteristic times) or the decrease of the quasielastic intensity (i.e. fewer mobile groups) on increasing the cross-linking molar ratio. To discriminate between these alternative situations and to get quantitative information we analysed the spectra by the model described in the “Theoretical background” section. The experimental quasielastic signal can be well described as a sum of Lorentzian functions convoluted with the instrumental resolution function.

In particular, the spectra of CDNS have been adequately reproduced by using only one Lorentzian component, $L(\sigma, \omega)$ with linewidth σ , describing the sub-meV broadening of the elastic peak and a flat background⁴⁹. In Fig. 5, a typical example of best fitting procedure of $S_{QE}(Q, \omega)$ is shown for β -CDPMA12 at two different values of exchanged momentum Q .

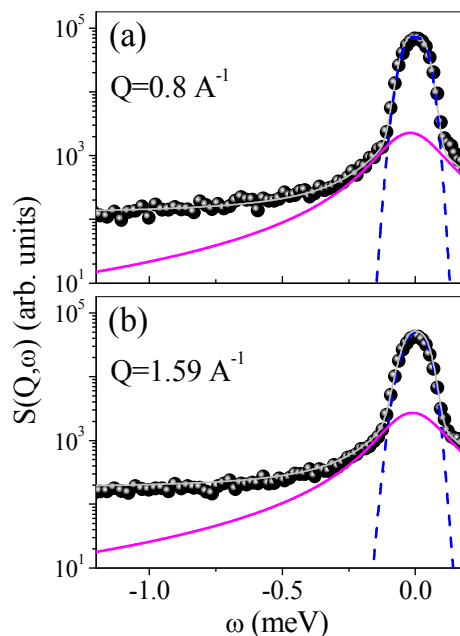
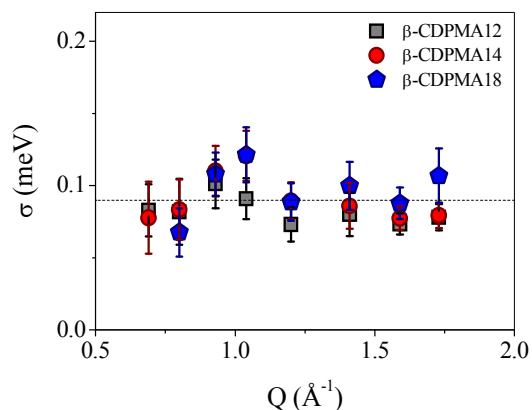


Figure 5: Typical example of best fitting results for quasi elastic neutron intensity of β -CDPMA12 at $Q=0.8 \text{ \AA}^{-1}$ (a) and $Q=1.59 \text{ \AA}^{-1}$ (b). Symbols:

experimental data; continuous magenta line: lorentzian component, dashed blue line: resolution. The error bars are not reported for sake of clarity.

- 5 The Q-dependence of the line width σ of the Lorentzian function used to reproduce the quasielastic signal gives information on the dynamic of the atoms inside the volume explored by the moving protons.



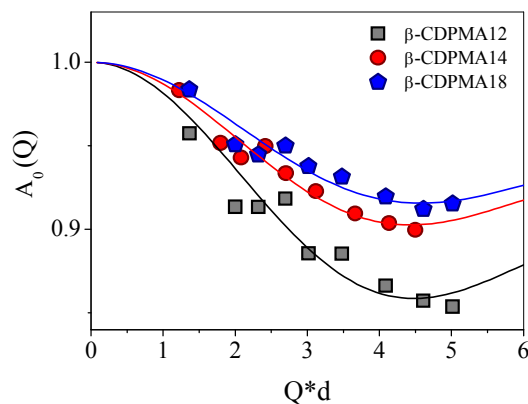
10 **Figure 6:** Linewidth (fwhm) σ of the Lorentzian contribution quasielastic neutron scattering as a function of Q for β -CDPMA1 n nanosponges ($n=2, 4$ and 8) at $T=300\text{K}$.

In Fig. 6, the line widths obtained by fitting procedure of the experimental quasielastic contribution are reported as a function of Q for β -CDPMA1 n nanosponges.

The characteristic time of the motions which give rise to the quasi-elastic signal is found to be quite similar for all the three types of examined polymers and it is about 7.3 ps.

20 The independence on Q of the half-width of $L(\sigma, \omega)$ (see Fig. 6) suggests that the hydrogen atoms of the polymer network of nanosponges explore a finite volume, i.e. their dynamics is confined^{49,50}. Indeed, this signature of a confined motion holds in the experimental accessible timescale that is estimated as the inverse of the energy resolution corresponding to about 15ps. In fact, a more detailed treatment of confined motions, accounting also for the dynamical behaviour over longer timescale may even give rise to Q -dependent splitting⁵¹. [Bickel 2002]

30 More detailed information on the geometry of the proton motions of the system are provided by the calculated elastic incoherent structure factor $A_0(Q)$ which show a different Q -behaviour for the three β -CDPMA1 n nanosponges, as evident in Fig. 7.



35 **Figure 7:** Q -dependence of $A_0(Q)$ for β -CDPMA1 n nanosponges ($n=2, 4$ and 8) at $T=300\text{K}$. The error bars (less than 5%) are not reported for sake of clarity.

In order to obtain more quantitative details on the dynamics of the three different samples of nanosponges, the experimental profiles of $A_0(Q)$ can be well described by using the same double-well jump model previously adopted for the analysis of elastic intensities (eq. (2)).

Consistently with the Q -independent behaviour of the linewidths σ , we assume that most of the diffusing hydrogen atoms belong to OH groups of CD and they can perform a random jump diffusion motion between two sites separated by the characteristic distance d . Based on these assumptions, the elastic incoherent structure factor $A_0(Q)$ can be well reproduced by using eq. (2), as shown in Fig. 7 for the three different types of examined nanosponges.

The fitting procedure of $A_0(Q)$ provides the estimation of the parameter $f = 1 - 4p_1p_2$ which represents the fraction of atoms that move too slowly to be resolved in the experiment.

55 The values obtained for the “immobile” atoms f are reported in Table 2 together with those found for the characteristic distance d between the sites among which the mobile hydrogens diffuse by random jump (Table 2).

Type of nanosponge	f	d (Å)
β -CDPMA12	0.768 ± 0.04	2.9 ± 0.03
β -CDPMA14	0.840 ± 0.04	2.6 ± 0.02
β -CDPMA18	0.861 ± 0.04	2.9 ± 0.03

60 **Table 2:** Estimated values of fraction of immobile atoms f and distance d as obtained by the fit of elastic incoherent structure factor with eq. (2) for β -CDPMA1 n nanosponges ($n=2, 4$ and 8).

The increases of the fraction f of immobile hydrogens in CDNS at high values of the parameter n is fully consistent with the hypothesis that the molecular dynamics of nanosponges is mainly driven by the motion of the hydrogen atoms belonging to the OH group of CD. As a matter of fact, these groups are expected to be those involved in the reaction of polymerization with the cross-linked agent during the formation of the CD polymer network.

70 The characteristic distance of the jump diffusion motion is found quite similar for all the β -CDPMA1 n nanosponges and corresponding to an average value of 2.8 Å. This estimated value is consistent with the diffusion by jump motion from one OH group to another over the hydrogen bond pattern established inside the nanosponges polymer network.

Conclusions

The thermal fluctuations occurring in an innovative class of chemically cross-linked polymers of cyclodextrins have been investigated, on the picosecond timescale, through elastic and quasi elastic neutron scattering experiments. The comparative assessment of the fast molecular dynamics of hydrogen atoms in CD-polymers and in the single monomeric unit β -cyclodextrin has been performed with the aim to understand the balance between covalent bonds and hydrogen bonds in defining the molecular architecture and rigidity of the whole polymer network.

As a main result, the extent of thermal fluctuations in nanosponges are found to be sensibly broader than those estimated in single cyclodextrin, revealing the establishment, in the polymer, of a characteristic inter-molecular HB network at the expense of the more strongly interconnected intra-molecular HB formed among OH groups on the rims of the macrocycle.

This finding, together with the description of the molecular diffusion dynamics in the polymer network provided by the

analysis of the elastic incoherent structure factor, suggests a picture in which the jump diffusion motion of more mobile hydrogen atoms over the hydrogen bond network of nanosponges dominates the dynamics of the system over the picosecond temporal window.

Finally, the molecular rigidity of CDNS related to the hampering of the picosecond time scale dynamics can be of great interest in order to optimize the design and synthesis of cyclodextrin-based polymers with tuneable inclusion/release properties for specific technological applications.

Acknowledgements

The authors gratefully acknowledge PRIN 2010-2011 NANOMED prot. 2010 FPTBSH for financial support and the reviewers for thorough and accurate revision of our paper and the suggestions.

Notes and references

^a Elettra - Sincrotrone Trieste, Strada Statale 14 km 163.5, Area Science Park, 34149 Trieste, Italy and Department of Physics University of Trento, via Sommarive 14, 38123 Povo, Trento, Italy Fax: +390461281690; Tel: +390461282940 E-mail: rossi@science.unitn.it

^b Department of Physics and Earth Sciences, University of Messina, Viale Ferdinando Stagno D'Alcontres 31, 98166 Messina, Italy

^c Department of Physics, University of Perugia, Via A. Pascoli, 06123 Perugia, Italy

^d Department of Chemistry, Materials and Chemical Engineering "G. Natta", Politecnico di Milano, Piazza L. da Vinci 32, 20133, Milano, Italy

^e Laboratoire Léon Brillouin (CEA/CNRS), CEA Saclay, 91191 Gif-sur-Yvette Cedex, France

^f CNR-IOM, c/o ILL, 71 avenue des Martyrs, CS 20156-38042, Grenoble, France

^g Department of Chemistry, University of Torino, Via Pietro Giuria 7, 10125 Torino, Italy

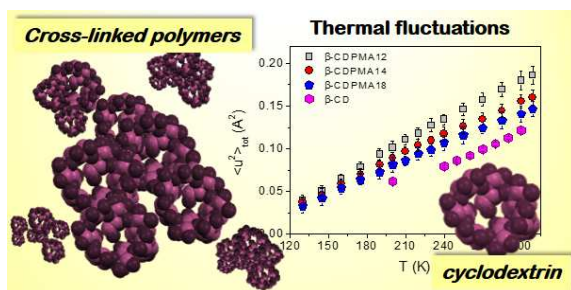
‡ Actually, the latter expression and the relationship for the double-well model mean square displacements describe one dimensional system motions. To pass to a 3D system one has to multiply the resulting MSD values by a factor of 3.

- 1 R. A. Dickie, S. S. Labana, Ronald S. Bauer, *Cross-Linked Polymers: Chemistry, Properties, and Applications (Acs Symposium Series)* American Chemical Society, 2nd Printing edition, 1988.
- 2 K. Sakurada, F.M. McDonald, F. Shimada, *Angew. Chem., Int. Ed.* 2008, **47** (31), 5718.
- 3 A. Atala, R.P. Lanza, J.A. Thomson, R.M. Nerem, R. M. *Principles of Regenerative Medicine*, Academic Press: Burlington, MA, 2008.
- 4 B.V. Slaughter, S.S. Khurshid, O.Z. Fisher, A. Khademhosseini, N.A. Peppas, *Adv. Mater.* 2009, **21**, 3307.
- 5 F. Trotta, M. Zanetti and R. Cavalli, *Beilstein J. Org. Chem.*, 2012, **8**, 2091.
- 6 S. Subramanian, A. Singireddy, K. Krishnamoorthy, M. Rajappan, *J. Pharm. Pharm. Sci.* 2012, **15** (1), 103.
- 7 D. Lembo, S. Swaminathan, M. Donalisio, A. Civra, L. Pastero, D. Aquilano, P. Vavia, F. Trotta, R. Cavalli, *Int. J. Pharm.* 2013, **443**, 262.
- 8 R. Minelli, R. Cavalli, L. Ellis, P. Pettazzoni, F. Trotta, E. Ciamporcerio, G. Barrera, R. Fantozzi, C. Dianzani, R. Pili, *Eur. J. Pharm. Sci.* 2012, **47**, 686.
- 9 S.J. Torne, K.A. Ansari, P.R. Vavia, F. Trotta, R. Cavalli, *Drug Delivery* 2010, **17**, 419.
- 10 D. Li, M. Ma, *Clean Prod. Processes* 2000, **2**, 112.
- 11 S. Swaminathan, L. Pastero, L. Serpe, F. Trotta, P.R. Vavia, D. Aquilano, M. Trotta, G. Zara, R. Cavalli, *Eur. J. Pharm. Biopharm.* 2010, **74**(2), 193.

- 12 E. Memisoglu-Bilensoy, I. Vural, A. Bochot, J. M. Renoir, D. Duchene, A. A. Hincal, *J. Controlled Release*, 2005, **104**, 489.
- 13 J. Szejtli, *Chem. Rev.* 1998, **98**, 1743.
- 14 M.L. Bender, M. Komiyama, *Cyclodextrin Chemistry*, Springer-Verlag, New York, 1978.
- 15 F. Castiglione, V. Crupi, D. Majolino, A. Mele, B. Rossi, F. Trotta and V. Venuti, *J. Phys. Chem. B*, 2012, **116**(43), 13133.
- 16 F. Castiglione, V. Crupi, D. Majolino, A. Mele, W. Panzeri, B. Rossi, F. Trotta and V. Venuti, *J. Incl. Phenom. Macrocycl. Chem.*, 2013, **75**(3-4), 247
- 17 B. Rossi, S. Caponi, F. Castiglione, S. Corezzi, A. Fontana, M. Giarola, G. Mariotto, A. Mele, C. Petrillo, F. Trotta and G. Viliani, *J. Phys. Chem. B*, 2012, **116** (17), 5323.
- 18 A. Mele, F. Castiglione, L. Malpezzi, F. Ganazzoli, G. Raffaini, F. Trotta, B. Rossi, A. Fontana and G. Giunchi, *J. Incl. Phenom. Macrocycl. Chem.*, 2011, **69**, 403.
- 19 F. Castiglione, V. Crupi, D. Majolino, A. Mele, B. Rossi, F. Trotta and V. Venuti, *J. Phys. Chem. B*, 2012, **116**(27), 7952.
- 20 V. Crupi, D. Majolino, A. Mele, B. Rossi, F. Trotta and V. Venuti, *Soft Matter*, 2013, **9**, 6457.
- 21 F. Castiglione, V. Crupi, D. Majolino, A. Mele, B. Rossi, F. Trotta and V. Venuti, *J. Raman Spectrosc.*, 2013, **44** (10), 1463.
- 22 V. Crupi, A. Fontana, D. Majolino, A. Mele, L. Melone, C. Punta, B. Rossi, F. Rossi, F. Trotta, V. Venuti *J. Incl. Phenom. Macrocycl. Chem.*, 2014, 2014, **80**, 69.
- 23 V. Crupi, A. Fontana, M. Giarola, S. Longeville, D. Majolino, G. Mariotto, A. Mele, A. Paciaroni, B. Rossi, F. Trotta, V. Venuti, *J. Phys. Chem. B*, 2014, **118**(2), 624.
- 24 V. Crupi, A. Fontana, M. Giarola, D. Majolino, G. Mariotto, A. Mele, L. Melone, C. Punta, B. Rossi, F. Trotta and V. Venuti, *J. Raman Spectrosc.*, 2013, **44** (10), 1457.
- 25 V. Crupi D. Majolino, A. Mele, L. Melone, C. Punta, B. Rossi, F. Toraldo, F. Trotta, V. Venuti, *Soft Matter*, 2014, **10**, 2320.
- 26 F. Castiglione, V. Crupi, D. Majolino, A. Mele, L. Melone, W. Panzeri, C. Punta, B. Rossi, F. Trotta, V. Venuti, *J. Incl. Phenom. Macrocycl. Chem.*, 2014, 2014, **80**, 77.
- 27 W. Liang, C. Yang, D. Zhou, H. Haneoka, M. Nishijima, G. Fukuhara, T. Mori, F. Castiglione, A. Mele, F. Caldera, F. Trotta and Y. Inoue, *Chem. Commun.*, 2013, **49**, 3510.
- 28 B. Rossi, A. Fontana, M. Giarola, G. Mariotto, A. Mele, C. Punta, L. Melone, F. Toraldo, F. Trotta, *J. Non Cryst. Solids*, 2014, **401**, 73.
- 29 F. Trotta and W. Tumiatti, *Cross-linked polymers based on cyclodextrin for removing polluting agents*; Patent WO 03/085002, 2003.
- 30 F. Trotta, W. Tumiatti, R. Cavalli, O. Zerbinati, C.M. Roggero and R. Vallero, *Ultrasound-assisted synthesis of cyclodextrin-based nanosponges*; Patent number WO 06/002814, 2006.
- 31 F. Trotta, V. Tumiatti, R. Cavalli, C. Rogero, B. Mognetti and G. Berta, *Cyclodextrin-based nanosponges as a vehicle for antitumoral drugs*; Patent number WO 09/003656 A1, 2009.
- 32 R., Lefort, D. Morineau, R. Guégan, C. Ecolivet, M. Guendouz, J.M. Zanotti, B. Frick, *Phys. Chem. Chem. Phys.* 2008, **10**, 2993.
- 33 J.C.Q. Smith, *Rev. Biophys.* 1991, **24**, 1.
- 34 K. Wood, A. Frolich, A. Paciaroni, M. Moulin, M. Hartlein, G. Zaccai, D.J. Tobias, M. Weik, *J. Am. Chem. Soc.* 2008, **130**, 4586.
- 35 M. Plazanet, M. Dean, M. Merlini, A. Huller, H. Emerich, C. Meneghini, M.R. Johnson, H.P. Trommsdorff, *J. Chem. Phys.* 2006, **125**, 154504.
- 36 F. Sonvico, M.T. Di Bari, L. Bove, A. Deriu, F. Cavatorta, G. Albanese, *Physica B* 2006, **385-386**, 725.
- 37 A. Stoeckli, A. Furrer, C. Schoenenberger, B.H. Meier, R.R. Ernst, I. Anderson, *Physica B* 1986, **136**, 161.
- 38 W. Doster, S. Cusack, W. Petry, *Nature* 1989, **337**, 754.
- 39 B. Frick, D. Richter, *Science* 1995, **267**, 1939.
- 40 P. W. Fenimore, H. Frauenfelder, B.H. McMahon, R. D. Young, *Proc. Natl. Acad. Sci. U.S.A.* 2004, **101**, 14408.
- 41 M. Bée, *Quasielastic Neutron Scattering*. Adam Hilger, Bristol, UK, 1988

-
- 42 J. Fitter, R.E. Lechner, N.A. Dencher, *Biophys. J.* 1997, **73**,
2126.
- 43 T. Springer, *Quasielastic Neutron Scattering for
the Investigation of Diffusive Motions in Solids and Liquids*,
Springer Tracts in Modern Physics; Springer: Berlin, 1972.
- 5 44 A. Paciaroni, S. Cinelli, G. Onori, *Biophys. Journal* 2002, **83**,
1157.
- 45 S. Magazù, G. Maisano, F. Migliardo, A. Benedetto, *J. Phys.
Chem. B* 2008, **112**, 8936.
- 10 46 V. Crupi, D. Majolino, A. Paciaroni, R. Stancanelli, V. Venuti,
J. Phys. Chem. B 2009, 113, 11032.
- 47 G. Zaccai, *G. Science* 2000, **288**, 1604.
- 48 D. G. Bicoût, G. Zaccai, *Biophys. J.* 2001, **80**, 1115.
- 49 V. Crupi, G. Guella, S. Longeville, D. Majolino, I. Mancini,
15 A. Paciaroni, B. Rossi, V. Venuti, *J. Phys. Chem. B* 2013, **117**,
11466.
- 50 V.F. Sears, *Can. J. Phys.* 1967, **45**, 237.
- 51 T. Bickel, C.M. Marques, *Eur. Phys. J. E* 2002, **9**, 349.

20



The thermal fluctuations and the relaxational dynamics in cyclodextrin based cross-linked polymers are explored by elastic and quasi-elastic neutron scattering.